SPECTROSCOPY
OF CONDENSED PHASES

Study of the Surface Morphology, Electrophysical Characteristics, and Photoluminescence Spectra of GaAs Epitaxial Films on GaAs(110) Substrates

G. B. Galiev[a], E. A. Klimov[a], A. A. Zaitsev[b], S. S. Pushkarev[a], *, and A. N. Klochkov[a]

[a] Mokerov Institute of Ultrahigh Frequency Semiconductor Electronics, Russian Academy of Sciences, Moscow, 117105 Russia
[b] National Research University "MIET", Zelenograd, Moscow, 124498 Russia
* e-mail: s_s_e_r_p@mail.ru
Received December 17, 2019; revised January 15, 2020; accepted February 28, 2020

Abstract—The electrophysical and phosphorescence characteristics, as well as the surface morphology, of GaAs films grown by molecular beam epitaxy on GaAs substrates with the (110) crystallographic orientation are studied. The silicon-doped epitaxial layers were grown at temperatures from 410 to 680°C with arsenic-to-gallium flux ratios from 14 to 84. The ranges of the growth conditions for obtaining the smoothest epitaxial film surface are determined by atomic force microscopy. The behavior of silicon atoms in GaAs is interpreted using analysis of the photoluminescence spectra of the grown samples taking into account that silicon atoms occupy Ga or As sites, i.e., taking into account the appearance of Si_{Ga} and Si_{As} point defects, as well as of arsenic and gallium vacancies V_{As} and V_{Ga}.

INTRODUCTION

The A^3B^5 semiconductor compounds epitaxially grown on substrates with the (100) crystallographic orientation are most widely used in modern microelectronics and best studied. This is partly related to the fact that molecular beam epitaxy (MBE) allows one to rather easily grow a large number of various structures on these substrates for different applications. However, in recent years interest has grown in structures grown on substrates with (111) and (110) orientations. The delay in the application of these substrates is caused by the relatively narrow range of technological conditions of epitaxial growth on these substrates in comparison with the growth on (100) substrates [1]. The main growth parameters are (i) growth temperature, (ii) partial pressure ratio of the III and V group elements, and (iii) growth rate. However, it was shown in recent years that semiconductor structures grown on (111)A and (110) substrates are promising for creating a new generation of field transistors, as well as of original quantum-well structures, topological insulators, etc. [1]. In addition, structures on (111)A and (110) substrates possess a built-in piezoelectric field directed vertically or lying in the growth plane [2–4]. This circumstance affects not only the mechanism and specific features of epitaxial growth, but also the fun-

damental properties of the grown structures [1]. It is also well known that silicon as a doping impurity exhibits pronounced amphoteric properties in GaAs epitaxial films grown on (111)A and (110) GaAs substrates. On these substrates, it is possible to grow GaAs:Si epitaxial films with both *n*- and *p*-type conductivity, as well as compensated insulating films [5–9], by using different growth conditions.

The aim of the present work is to study the surface morphology, conductivity type, and charge carrier concentration, as well as the photoluminescence (PL) spectra, of uniformly silicon-doped GaAs epitaxial films grown on GaAs(110) substrates in the temperature range of 410–680°C.

SAMPLES AND METHODS
OF THEIR INVESTIGATION

The samples under study were grown by the MBE method of semi-insulating GaAs(110), (111)A, and (100) substrates. The films on GaAs(100) and (111)A substrates served as reference samples because the literature contains a lot of data on these structures. To achieve the highest identity of the technological growth parameters, namely, growth temperature (T_g), partial pressure ratios of arsenic tetramers As_4 and gal-

lium atoms Ga (γ), and pregrowth treatment, three samples on pieces of GaAs(110), (111)A, and (100) substrates were grown in each growth process. The pieces of substrates were glued with indium to a molybdenum holder. The holder with the glued samples was annealed in a growth chamber in an As$_4$ flow at a temperature of up to 670°C before each growth process. After this, we first grew an undoped GaAs buffer layer 135 nm thick and then a silicon-doped GaAs:Si layer 675 nm thick. The growth rate was 90 Å/min. The silicon cell temperature in this case was 1080°C, which, under our conditions, corresponded to a conduction electron concentration of 1×10^{18} cm^{-3} under standard conditions of growth on GaAs(100) substrates. The samples were grown at different temperatures T_g in the range from 410 to 680°C, while γ varied within the range of 14−84. Growth temperature T_g were measured and controlled using a thermocouple mounted in the sample holder.

The electrophysical characteristics (mobility and concentration of charge carriers) were determined by measuring the specific resistance and the Hall effect by the four-probe method in the van der Pauw geometry at temperatures of 300 and 77 K in the dark. The PL spectra were measured in a combined optical cryostat in nitrogen vapors at 77 K. The PL was excited by focused radiation of a solid-state laser with a wavelength of 409 nm and a power of ~200 mW. The PL signals in the region of 1.2−2.0 eV were detected by a nitrogen-cooled FEU-62 photomultiplier. The energy resolution of the setup was 5 meV.

The surface roughness of samples was measured using an NT-MDT SolverPro atomic force microscope (AFM) in a contact regime.

ELECTROPHYSICAL PROPERTIES

Table 1 presents the film growth conditions and the results of measuring the conductivity type, mobility, and concentration of charge carriers, as well as the root-mean-square surface roughness R_q for three different orientations of substrates. The samples in Table 1 are listed in order of increasing growth temperature from 410 to 680°C. Parameter R_q was measured only for GaAs films with orientation (110) and calculated over the field 10×10 µm in size.

To test the quality of the i-GaAs buffer layer, we have grown additional structures, i.e., undoped GaAs layers 135 nm thick on the three types of substrates. The pregrowth treatment of substrates and the growth conditions of these additional structures corresponded to the samples studied. We used growth temperatures of 480, 510, 540, and 580°C. The Hall measurements showed that the buffer layers are highly resistive independently of the growth conditions. Thus, the undoped buffers grown at different temperatures did not contribute to the measured concentrations and

mobility of charge carriers for the samples presented in Table 1.

As is known from the literature, it is technologically difficult or even impossible to obtain simultaneously high electrophysical parameters and a smooth surface of films on GaAs(111)A and (110) substrates [5]. The surface morphology is a criterion for determining the growth conditions for obtaining high-quality epitaxial films. However, the doping efficiency in this case may be not very high.

The amphoteric nature of Si atoms is especially pronounced in the case of doping of structures on GaAs(111)A and (110) substrates. The conductivity type of epitaxial films on GaAs(111)A substrates in the case of a chosen growth temperature usually changes with changing γ. Under conditions of As deficiency, the p-type conductivity forms at low γ, the compensated material grows at intermediate γ, and the n-type conductivity forms at high γ [5, 10]. In the general case of simultaneous changes in T_g and γ, the conductivity type changes depending on these both parameters [11]. Despite the extensive study of the surface morphology and the behavior of Si atoms as a doping impurity on (n11)A-oriented substrates, the values of T_g and γ at which the conductivity type changes are different in works [5, 10−14]. The same situation is typical for the (110) orientation [8, 9, 15].

As is seen from Table 1, the uniformly silicon-doped samples on GaAs(100) substrates have only the n-type conductivity or are highly resistive in the case of a decrease in the growth temperature (samples 72, 83, 75). The samples on GaAs(111)A substrates have only the p-type conductivity (samples 80 and 87) or are compensated.

Let us consider the electrophysical properties of GaAs(110) samples. The GaAs:Si(110) films have the n-type conductivity at growth temperatures $T_g >$ 460°C and intermediate γ ($\gamma = 40-60$). It should be noted that the type, mobility, and concentration of charge carriers in the case of the (110)-oriented substrate are functions of the flux of arsenic molecules. In particular, the concentration and mobility of electrons in the series of four samples grown at $T_g = 480$°C monotonically increase as γ increases from 14 to 42. However, sample 90, which is grown with $\gamma = 84$, is insulating. In the series of samples grown at $T_g = 580$°C, the p-type conductivity (sample 87) at low γ ($\gamma = 16$) changes to the n conductivity as γ increases to 58 (sample 73). At the same time, both sample 75 grown at intermediate $\gamma = 25$ and sample 76 grown with high $\gamma = 80$ are semi-insulating.

Thus, the electrophysical properties of epitaxial GaAs:Si(110) films strongly depend on the growth conditions, namely, at each fixed growth temperature, there exists a narrow range of γ in which the grown films have the n-type conductivity with high concentrations and mobilities of electrons. With decreasing γ, Si atoms begin to occupy acceptor sites in the GaAs

Table 1. Technological growth parameters (growth temperature T_g, As-to-Ga flux ratio γ), electrophysical parameters (type, concentration, and mobility of charge carriers) of samples at temperatures of 300 and 77 K, and root-mean-square roughness of their surfaces R_q

| Sample no.	T_g, °C	γ	Substrate orientation	Conductivity type	R_q, nm	Mobility, cm²/(V s)		Concentration, cm⁻³	
						300 K	77 K	300 K	77 K
72	410	55	(110)	—	5.2	—	—	—	
			(111)A	—		—	—	—	
			(100)	—		—	—	—	—
71	460	53	(110)	n	5.8	230	—	4.5×10^{16}	—
			(111)A	—		—	—	—	—
			(100)	n		214	52	5.5×10^{16}	5.2×10^{16}
91	480	14	(110)	n	8.4	300	100	2.8×10^{17}	3.0×10^{17}
			(111)A	—		—	—	—	—
			(100)	—		—	—	—	—
88	480	24	(110)	n	5.5	620	490	3.7×10^{17}	3.8×10^{17}
			(111)A	—		—	—	—	—
			(100)	—		—	—	—	—
84	480	42	(110)	n	3.6	1140	895	4.3×10^{17}	4.5×10^{17}
			(111)A	—		—	—	—	—
			(100)	—		—	—	—	—
90	480	84	(110)	—	4.2	—	—	—	—
			(111)A	—		—	—	—	—
			(100)	—		—	—	—	—
70	510	46	(110)	n	8.5	227	100	1.3×10^{17}	1.4×10^{17}
			(111)A	—		—	—	—	—
			(100)	n		580	340	2.5×10^{17}	2.9×10^{17}
83	550	42	(110)	n	15.3	430	360	3.5×10^{17}	3.6×10^{17}
			(111)A	—		—	—	—	—
			(100)	—		—	—	—	—
87	580	16	(110)	p	117	51	77	4.3×10^{17}	1.1×10^{17}
			(111)A	p		60	48	6.0×10^{17}	2.5×10^{17}
			(100)	n		2250	2130	1.0×10^{18}	1.1×10^{18}
75	580	25	(110)	—	12.3	—	—	—	—
			(111)A	—		—	—	—	—
			(100)	—		—	—	—	—
73	580	58	(110)	n	15.5	1040	850	2.5×10^{17}	2.5×10^{17}
			(111)A	—		—	—	—	—
			(100)	n		1475	1150	3.8×10^{17}	3.8×10^{17}
76	580	80	(110)	—	21.9	—	—	—	—
			(111)A	—		—	—	—	—
			(100)	n		290	95	2.3×10^{16}	2.2×10^{16}
74	620	58	(110)	n	11.1	2390	2130	5.6×10^{17}	5.6×10^{17}
			(111)A	—		—	—	—	—
			(100)	n		2000	1800	5.3×10^{17}	5.3×10^{17}
80	680	44	(110)	n	51.3	690	560	3.9×10^{17}	3.9×10^{17}
			(111)A	p		209	378	4.9×10^{17}	1.0×10^{17}
			(100)	n		2850	2480	6.0×10^{17}	6.3×10^{17}

crystal lattice. Therefore, the GaAs:Si film conductivity changes from *n* to *p* type through the insulating compensated state. As γ increases to 80, the GaAs:Si(110) films grown at T_g = 480 and 580°C become insulating. The range of optimal γ for the samples with the *n*-type conductivity is, most probably, a function of the growth temperature similar to the case with (111)A substrates. In particular, the concentration and mobility of electrons in sample 80 grown at high temperature T_g = 680°C are lower than in sample 74 (T_g = 620°C).

SURFACE MORPHOLOGY OF SAMPLES

The morphology was studied with an AFM only for samples with the (110) orientation. Figure 1 shows the AFM images of the surfaces of samples grown at different temperatures T_g with intermediate ratios of As$_4$ and Ga pressures γ = 40−60. As is seen, the surface of samples grown at high T_g (samples 80 and 74) is rough and contains a lot of triangular pyramids oriented along the [001] direction. Surface faceting is typical in the case of epitaxial growth of GaAs(110) under the growth conditions close to optimal for (100) substrates [16]. The pyramids at T_g = 680°C are several micrometers in size. With a decrease in the growth temperature from 680 to 620°C and a slight decrease in γ, the shape of pyramids considerably changes, namely, the angle of the [001] vertex decreases and the vertices become truncated and smoothened. In addition, the pyramids decrease in size and the root-mean-square roughness decreases approximately fivefold. Further decrease in T_g from 620 to 550−580°C leads to a more complex morphology, i.e., to formation of faceted mounds of different shapes, which are oriented mainly along the [001] direction and separated by deep dimples. The surface roughness (samples 73, 76, and 83) under these conditions is 15−20 nm.

At γ = 40−60 and a temperature decreased to 510°C and lower, the surface roughness considerably decreases to R_q < 9 nm. The surface of these films contains mounds and dimples of irregular shapes independent of the [001] or [$\bar{1}$10] crystallographic directions of the (110) substrate.

Figure 2 presents the AFM images of the surface of GaAs:Si (110) films for two series of four samples grown at fixed temperatures T_g = 480 or 580°C with different γ. Figure 2 allows us to judge the influence of γ on the surface morphology of GaAs:Si films. Samples 87, 75, 73, and 76 were grown at T_g = 580°C. The surface of sample 87 contains multiple elliptical objects. Most probably, Ga droplets form on the (110) growth surface under the condition of As$_4$ deficiency and then crystallize in GaAs upon cooling of the structure. Similar formation of droplets was observed in [17]. The surface of sample 75 (γ = 25) consists of overlapping triangular pyramids. One of the angles of
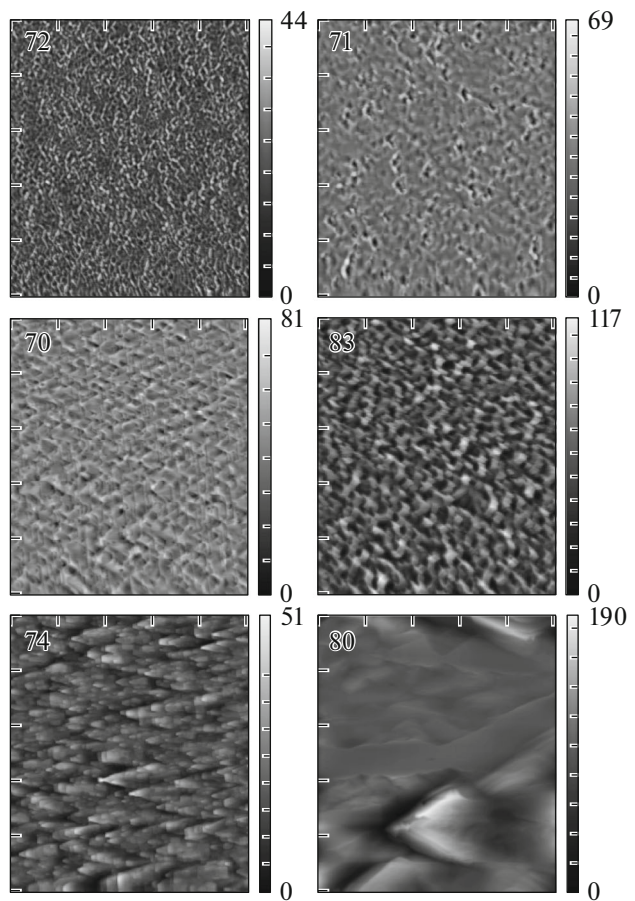
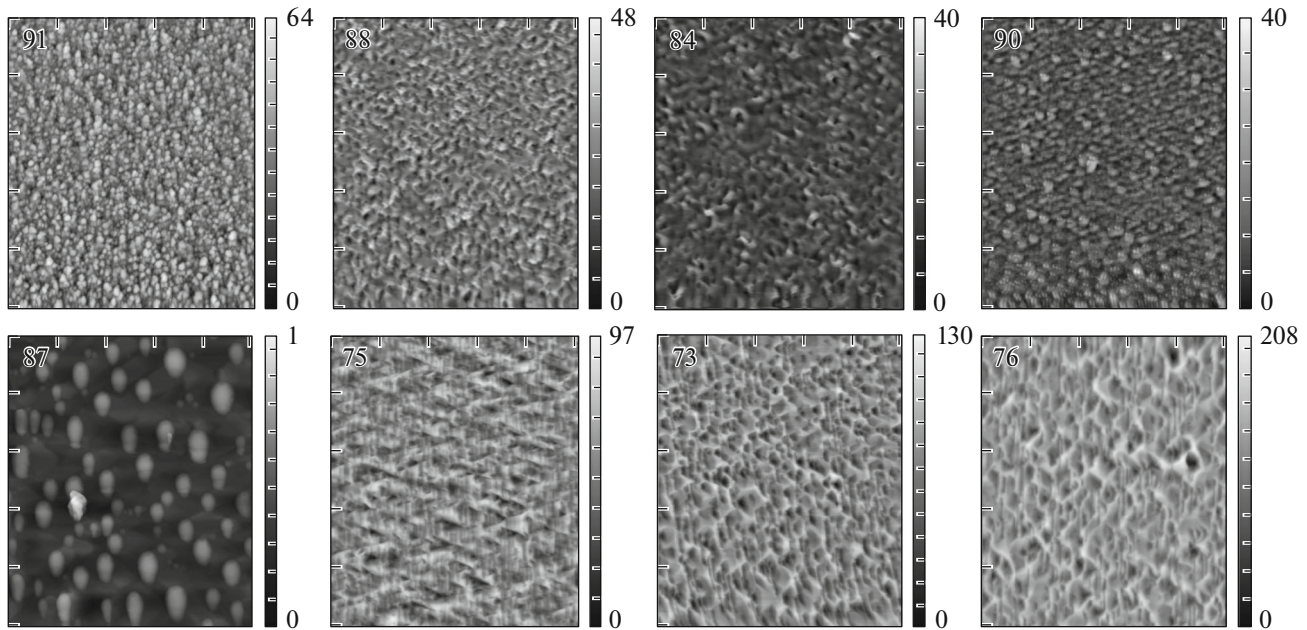**Fig. 1.** AFM images of surfaces of GaAs:Si(110) films grown at different temperature T_g and intermediate pressure ratios γ = 40−60. The scan field size is 10 × 10 μm; the height scale is in nanometers. The [001] direction is horizontal.

the pyramid base is oriented in the [001] direction, and the opposite edge of the base is parallel to [1$\bar{1}$0]. With increasing γ, the surface of samples begins to consist of steps and dimples.

The surfaces of samples grown at a temperature of 480°C (Fig. 2, upper row) contain no faceted or oriented forms. The lowest surface roughness is demonstrated by sample 84 (R_q = 3.6 nm) grown at γ = 42. The concentration and mobility of electrons in this sample are also the highest in the considered series of samples.

Electrophysical parameters μ and *n* indicate the quality of the grown epitaxial films. The best sample from this viewpoint is sample 84, which has the highest mobility of charge carriers and the lowest surface roughness. This allows us to conclude that the growth conditions of this sample with *n* conductivity (T_g = 480°C, γ = 42) are the best for GaAs(110) substrates. The decrease in the growth temperature to 410°C results in a relatively weak increase in the surface roughness to 5.2 nm (sample 72). The increase in T_g

Fig. 2. AFM images of surfaces of GaAs:Si(110) films grown at different γ. The samples in the upper and lower rows are grown at T_g = 480 and 580°C, respectively; γ increases from left to right. The scan field size is 10×10 μm (20 × 20 μm for sample 87). The height scale is in nanometers (in micrometers for sample 87). The [001] direction is horizontal.

from 480 to 680°C causes a stronger increase in the surface roughness (Tables 1 and 2).

The structures with p-type conductivity on GaAs(110) (sample 87) exhibit a considerable increase in the root-mean-square surface roughness up to 117 nm. Thus, to grow structures with the p-type conductivity on GaAs(110) substrates with a relatively good surface morphology, it is necessary to perform additional optimization of the epitaxial growth regime. Upward or downward deviations from 480°C lead to an increase in the surface roughness. Therefore, the growth temperature of 480°C in combination with γ = 42–55 is optimal for growing smooth epitaxial films on GaAs(110) substrates.

PHOTOLUMINESCENCE SPECTRA

As was mentioned above, the growth of epitaxial films with a good morphology and n or p conductivity on GaAs(110) substrates is a hard task. Due to a higher Si dopant self-compensation coefficient in GaAs(110) than in GaAs(100) and (111), it is often difficult to obtained a smooth surface of Si-doped layers grown by MBE on GaAs(110). As a rule, one has to compromise in each particular case. To achieve the best morphology, it is necessary to change the growth technological parameters, which, in turn, have a complex effect on the Si dopant self-compensation coefficient [8, 9] and, hence, on the concentration of charge carriers.

All the aforementioned problems of MBE on GaAs(110) are related to the specific features of the surface. While the epitaxial layers on GaAs(100) and (111) consist of alternating planes of Ga and As atoms, the GaAs(110) surface consists of identical numbers of Ga and As atoms [18]. The Ga and As atoms on the (110) surface have a single free bond (three bonds are directed into the volume). The configuration of the atomic bonds of Ga is the same for the (110) and

Table 2. Components of the PL spectra of samples under study (Gaussian peak energy $\hbar\omega$, Gaussian width at half maximum $\Delta\hbar\omega$, and area under the Gaussian S)

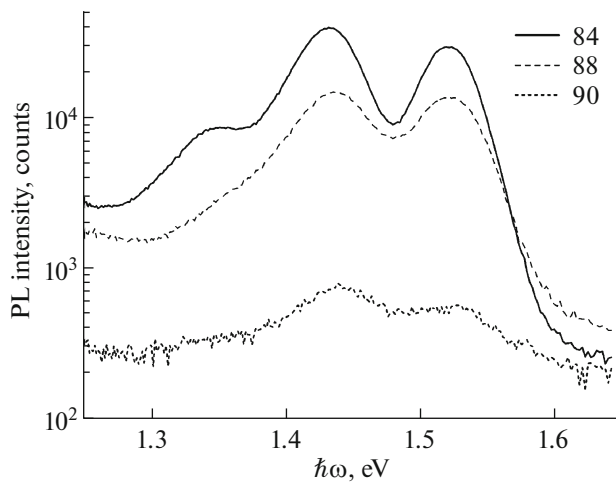| Sample no., surface orientation	Gaussian 1			Gaussian 2			Gaussian 3			Gaussian 4		
	$\hbar\omega_1$, eV	$\Delta\hbar\omega_1$, eV	S_1, arb. units	$\hbar\omega_2$, eV	$\Delta\hbar\omega_2$, eV	S_2, arb. units	$\hbar\omega_3$, eV	$\Delta\hbar\omega_3$, eV	S_3, arb. units	$\hbar\omega_4$, eV	$\Delta\hbar\omega_4$, eV	S_4, arb. units
84 (110)	1.521	0.040	1437	1.433	0.044	2017	1.358	0.081	819	1.247	0.053	130
88 (110)	1.521	0.046	756	1.438	0.051	835	1.378	0.062	175	0.37	1.24	8014
90 (110)	1.526	0.043	14.5	1.440	0.070	37.1	—	—	—	—	—	—

Fig. 3. PL spectra of samples 84, 88, and 90 at $T = 77$ K.

(111)A surfaces. In the process of formation of GaAs:Si films, Si and As atoms may compete for As sites of the crystal lattice. It is the small number of broken bonds of As atoms which increases the probability that Si atoms will substitute As atoms and, therefore, exhibit donor properties. Because of this, GaAs substrates with the (110) and (111)A orientations are similar with respect to the amphoteric nature of Si atoms in GaAs:Si films. On the other hand, the GaAs(110) surface is nonpolar, which substantially differs it from the (100) and (111)A surfaces and may affect the properties of GaAs:Si films. Thus, we should not expect precise coincidence of the specific features of the PL spectra of films on GaAs(110) with the data for GaAs(111)A and (100) from the literature.

To analyze the PL spectra, we chose samples 84, 88, and 90, which were grown at $T_g = 480°C$ at different γ, namely, at $\gamma = 42, 24, 84$. These samples were chosen due to the following reasons. First, according to [8, 9, 16], the growth temperature of 480°C lies within the region of most frequently used temperatures and, second, sample 84 has the lowest surface roughness among the samples grown. In addition, the range of γ for the chosen samples is rather wide.

Figure 3 shows the PL spectra of samples 84, 88, and 90. As is seen, the PL spectra differ not only in intensity, but also in shape. While the PL spectrum of sample 90 exhibits two broad bands, the PL spectrum of sample 84 contains three bands. The PL spectrum of sample 88 also contains two clear bands, but the low-energy band has a pronounced low-energy shoulder. To analyze the PL spectra, we used the well-known Gaussian decomposition method [11]. Table 1 presents the results of this decomposition. One can see that the PL spectrum of sample 90 is well described by two Gaussians with maxima at $\hbar\omega_1 = 1.52$ eV and $\hbar\omega_2 = 1.44$ eV, while the PL spectra of samples 84 and 88 are decomposed into four Gaussians with maxima

at $\hbar\omega_1 = 1.52$ eV, $\hbar\omega_2 = 1.43$ eV, $\hbar\omega_3 = 1.358$ and 1.378 eV for samples 84 and 88, and $\hbar\omega_4 = 1.24$ eV, which lies outside the range of our measurements. One more specific feature is that the intensity ratio of two bands I_2/I_1 increases with increasing γ.

To explain the dependence of PL spectra on γ, we use the model of defect reaction [19]

$$V_{As} \leftrightarrow V_{Ga} + Ga_{As},$$

which means that arsenic vacancy V_{As} transforms into a defect pair (gallium vacancy V_{Ga} and gallium atom at the arsenic site Ga_{As}) via a simple jump of gallium atom to the arsenic site. Since these defects are charged, the reaction is controlled by the Fermi level position. The simple jump of the Ga atom occurs mostly in n-type samples and transforms deep donor V_{As} into a pair of deep acceptors V_{Ga} and Ga_{As} [19].

Therefore, we can consider the situation with samples 84, 88, and 90 as follows.

Sample 88 was grown at a small γ. The concentration of V_{As} in this sample should be higher than in samples 84 and 90. At the same time, dissociation of molecules As_4, which is less efficient on the (111)A surface than on (100), will be identical for all the samples. And, upon doping of samples, Si atoms occupying V_{As} will behave as acceptors.

As is seen from Fig. 3, the PL spectra of all the samples contain bands at $\hbar\omega_1 = 1.52$ eV and $\hbar\omega_2 = 1.43$ eV. The first band is traditionally related to electron−hole recombination in n-GaAs. The data on the second band are contradictory, i.e., it is assigned to the transitions from the conduction band to the acceptor levels of intrinsic defects V_{Ga} and Ga_{As} or impurity defects Si_{As} [20, 21]. In any case, it is believed that the emission band at $\hbar\omega = 1.43$ eV corresponds to an elementary acceptor defect. As follows from [20], the intensity of the band at $\hbar\omega = 1.43$ eV for the (111)A surface is higher than for (100). Thus, we can suggest that, for our samples on (110) substrates, the main contribution to the emission intensity in this photon energy region is made by the region with (111)A. This follows from the stronger amphoteric behavior of Si on the (111)A than on the (100) surface. In addition, the intensity of this band turns out to be higher than the intensity of the main band with $\hbar\omega = 1.52$ eV. In our case, it is this situation which takes place for samples 84 and 90, while the intensities of these bands for sample 88 are approximately identical. Thus, with increasing As pressure (i.e., with increasing γ), among three defect types V_{Ga}, Ga_{As}, and Si_{As}, which can be responsible for the PL with $\hbar\omega = 1.43$ eV, Si_{As} is the most probable.

As is seen from Fig. 3 and Table 2, the PL spectra of samples 84 and 88 formed at low and intermediate γ contain a band with $\hbar\omega = 1.35-1.37$ eV. This band is not recorded in the PL spectrum of sample 90 due to, probably, its low intensity. The authors of [20, 22]

assigned a similar band for GaAs(100) at $\hbar\omega = 1.36$ eV to the $Si_{As}-V_{As}$ complex and noted that it is more often observed in samples with p-type conductivity or at low γ. However, the samples in our case have n-type conductivity. This means that the concentration of Si_{Ga} defects, which are responsible for the n conductivity, is rather high, and the contribution to the PL line from the (100) surface is dominant. Following the authors of [19], we relate the recorded change in the transition energy by 0.02 eV for samples 84 and 88 to a change in the bond energy of the Si_{As} acceptor.

Decomposition of the PL spectrum of sample 84 into Gaussians reveals a peak at $\hbar\omega = 1.24$ eV, which lies outside the range of PL recording. In [22], the peak at $\hbar\omega = 1.23$ eV for silicon-doped GaAs(100) was assigned to internal electronic transitions between the excited and ground states of the $Si_{Ga}-V_{Ga}$ complex. Since Si_{Ga} is a donor and V_{Ga} is a deep acceptor, they form a donor−acceptor pair. The authors of [19] discussed the PL band of GaAs(111)A with energy $\hbar\omega = 1.32$ eV, which shifts to $\hbar\omega = 1.28$ eV with decreasing photoexcitation power. In [23], this band was assigned to recombination from the charged Ga_{As}^{-} defect. The authors of [23] also note that the bands at $\hbar\omega = 1.32$ and 23 eV are related to Ga vacancies in charged states, namely, to V_{Ga}^{-} and V_{Ga}^{2-}, respectively. In our case, Ga vacancies at intermediate γ (i.e., for sample 84) can be formed due to insufficiently intense dissociation of As_4, which leads to jumping of Ga atoms from their sites to As sites.

CONCLUSIONS

We have studied the electrophysical parameters, surface morphology, and PL spectra of uniformly silicon-doped GaAs films grown by MBE on GaAs substrates with the (110) orientation. The growth temperature ranged from 410 to 680°C and γ varied from 14 to 84. It is found that the electrophysical properties and surface morphology of GaAs:Si epitaxial films strongly depend on the growth conditions. The samples with a high concentration and mobility of charge carriers are also characterized by a developed faceted surface morphology. The optimal set of characteristics was demonstrated by a sample grown at temperature $T_g = 480$°C and pressure ratio of As_4 molecules and Ga atoms $\gamma = 42$.

The PL spectra of GaAs:Si(110) layers exhibit, in addition to the main band at $\hbar\omega_1 = 1.52$ eV, bands at $\hbar\omega_2 = 1.43-1.44$ eV, $\hbar\omega_3 = 1.35-1.37$ eV, and $\hbar\omega_4 = 1.24$ eV, which are assigned to the Si_{As}, Si_{Ga}, V_{As}, and V_{Ga} point defects.

CONFLICT OF INTEREST

The authors declare that they have no conflict of interest.

REFERENCES

1. C. D. Yerino, B. Liang, D. L. Huffaker, P. J. Simmonds, and M. L. Lee, J. Vac. Sci. Technol. B **35**, 010801 (2017).
   https://doi.org/10.1116/1.4972049

2. D. Sun and E. Towe, Jpn. J. Appl. Phys. **33**, 702 (1994).
   https://doi.org/10.1143/JJAP.33.702

3. P. O. Vaccaro, K. Tominaga, M. Hosoda, K. Fujita, and T. Watanabe, Jpn. J. Appl. Phys. **34**, 1362 (1995).
   https://doi.org/10.1143/JJAP.34.1362

4. M. Ilg, K. H. Ploog, and A. Trampert, Phys. Rev. B **50**, 17111 (1994).
   https://doi.org/10.1103/PhysRevB.50.17111

5. T. Ohachi, J. M. Feng, K. Asai, M. Uwani, M. Tateuchi, P. O. Vaccaro, and K. Fujita, Microelectron. J. **30**, 471 (1999).
   https://doi.org/10.1016/S0026-2692(98)00155-4

6. G. B. Galiev, M. V. Karachevtseva, V. G. Mokerov, V. A. Strakhov, and N. G. Yaremenko, Dokl. Phys. **44**, 510 (1999).

7. G. Galiev, V. Kaminskii, D. Milovzorov, I. Velihovskii, and V. Mokerov, Semicond. Sci. Technol. **17**, 120 (2002).
   https://doi.org/10.1088/0268-1242/17/2/305

8. E. S. Tok, J. H. Neave, M. J. Ashwin, B. A. Joyce, and T. S. Jones, J. Appl. Phys. **83**, 4160 (1998).
   https://doi.org/10.1063/1.367169

9. T. C. Zhou, X. C. Zhou, and W. P. Kirk, J. Appl. Phys. **81**, 7372 (1997).
   https://doi.org/10.1063/1.365437

10. A. Miyagawa, T. Yamamoto, Y. Ohnishi, J. T. Nelson, and T. Ohachi, J. Cryst. Growth. **237−239**, 1434 (2002).
    https://doi.org/10.1016/S0022-0248(01)02235-7

11. G. B. Galiev, E. A. Klimov, A. N. Klochkov, S. S. Pushkarev, and P. P. Maltsev, Semiconductors **52**, 376 (2018).
    https://doi.org/10.1134/S1063782618030119

12. L. Pavesi, M. Henini, and D. Johnston, Appl. Phys. Lett. **66**, 2846 (1995).
    https://doi.org/10.1063/1.113449

13. K. Agawa, K. Hirakawa, N. Sakamoto, Y. Hashimoto, and T. Ikoma, Appl. Phys. Lett. **65**, 1171 (1994).
    https://doi.org/10.1063/1.112136

14. Y. Okano, M. Shigeta, H. Seto, H. Katahama, S. Nishine, and I. Fujimoto, Jpn. J. Appl. Phys. **29**, L1357 (1990).
    https://doi.org/10.1143/JJAP.29.L1357

15. D. Sun and E. Toweand, J. Cryst. Growth **132**, 166 (1993).
    https://doi.org/10.1016/0022-0248(93)90258-X

16. D. M. Holmes, E. S. Tok, J. L. Sudijono, T. S. Jones, and B. A. Joyce, J. Cryst. Growth **192**, 33 (1998).
https://doi.org/10.1016/S0022-0248(98)00449-7

17. W. I. Wang, J. Vac. Sci. Tech. B **1**, 630 (1983).
https://doi.org/10.1116/1.582567

18. Y. Takano, M. Lopez, T. Torihata, T. Ikei, Y. Kanaya, K. Pak, and H. Yonezu, J. Cryst. Growth **111**, 216 (1991).
https://doi.org/10.1016/0022-0248(91)90974-A

19. F. Piazza, L. Pavesi, M. Henini, and D. Johnston, Semicond. Sci. Technol. **7**, 1504 (1992).
https://doi.org/10.1088/0268-1242/7/12/014

20. I. A. Bobrovnikova, M. D. Vilisova, I. V. Ivonin, L. G. Lavrent'eva, V. V. Preobrazhenski, M. A. Putyato, B. R. Semyagin, S. V. Subach, and S. E. Toropov, Semiconductors **37**, 1047 (2003).
https://doi.org/10.1134/1.1610116

21. V. G. Mokerov, G. B. Galiev, Yu. V. Slepnev, and Yu. V. Khabarov, Semiconductors **32**, 1175 (1998).
https://doi.org/10.1134/1.1187586

22. Hong N. Ky and F. K. Reinhart, J. Appl. Phys. **83**, 718 (1998).
https://doi.org/10.1063/1.366743

23. L. Pavesi, Hong N. Ky, J. D. Ganiere, F. K. Reinhart, N. Baba-Ali, I. Harrison, B. Tuck, and M. Henini, J. Appl. Phys. **71**, 2225 (1992).
https://doi.org/10.1063/1.351120

Translated by M. Basieva